Electronic Supplementary Material (ESI) for Nanoscale.

Supplementary information

Inserting the Auxeticity into Graphene Oxide via the Bottom-up Strategy

Cong Sun[a], Zeyan Wang[a], Nana Tian[a], Mingqing Liao[d], Conglin Zhang[c], Qingfeng Guan[a], Erjun Kan[b,*], Jintong Guan[a,*]

[a] *School of Materials Science and Engineering, Jiangsu University, Zhenjiang, 212013, P. R. China*

[b] *Department of Applied Physics and Institution of Energy and Microstructure, Nanjing University of Science and Technology, Nanjing, Jiangsu 210094, P. R. China*

[c] *School of Material Science and Engineering, Yancheng Institute of Technology, Yancheng, 224051, P. R. China*

[d] *School of Materials Science and Engineering, Jiangsu University of Science and Technology, Zhenjiang 212003, China*

Section I: the properties of SL-C_2O

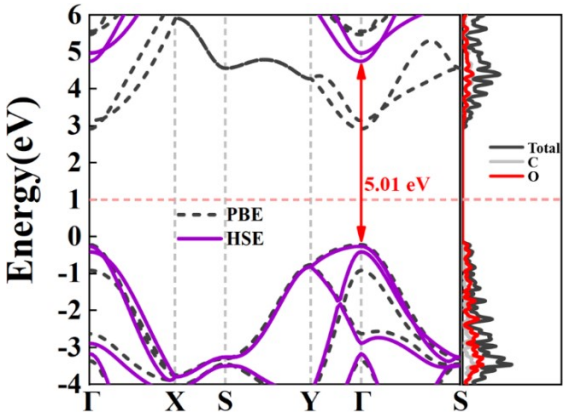

Fig. S1 The electronic structure of SL-C_2O.

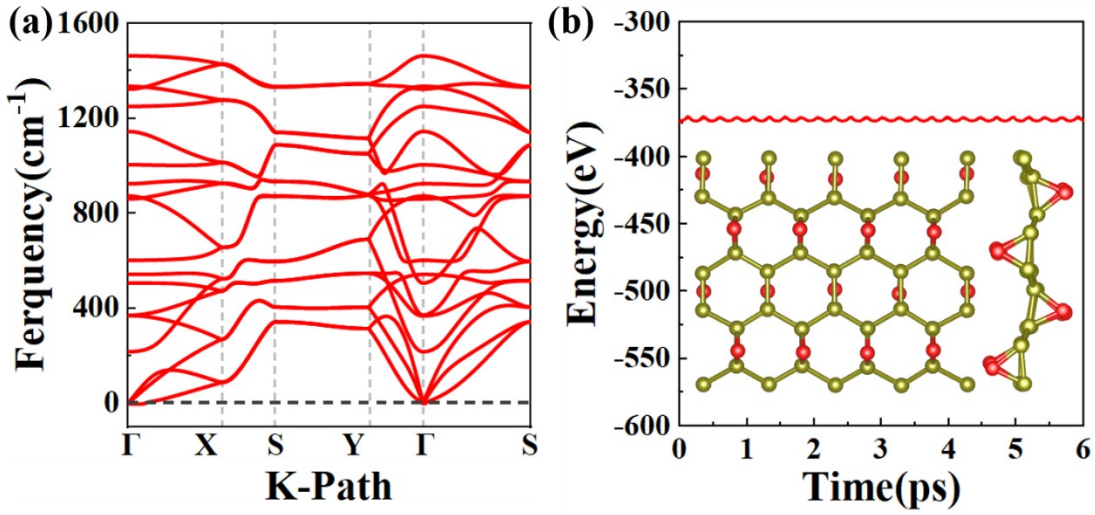

Fig. S2 The confirmation of stability of SL-C_2O. (a) the phonon dispersion curves and (b) The snapshots of ab initio molecular dynamics (AIMD) simulations at 300 K in 6ps.

Section II: the details of the four proposed stacking modes

The four staking modes is explained as below:

As shown in Fig. S3, α- is commonly known as the AA stacking, where all the atoms in two layers have same lateral coordinates. For β- phase, there is a relatively shift along the x-direction, where the hollow site (namely site 1) coordinates to the oxidized bridge site (namely site 2). For γ- phase, there is a bidirectional shift along both directions, where the oxidized bridge site (namely site 2) coordinates to the unoxidized bridge site (namely site 4). For δ- phase, the relatively shift is along the y-direction, where the oxidized bridge site (namely site 2) coordinates to the oxidized carbon atom (namely site 3).

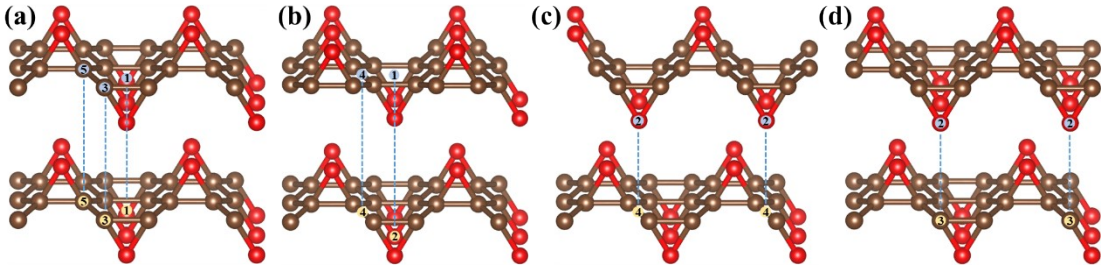

Fig. S3 The stacking modes of layer-stacking C_2O-based materials: (a) α-, (b) β-, (c) γ-, (d) δ-.

Section III: the dynamic stability of proposed C_2O-based

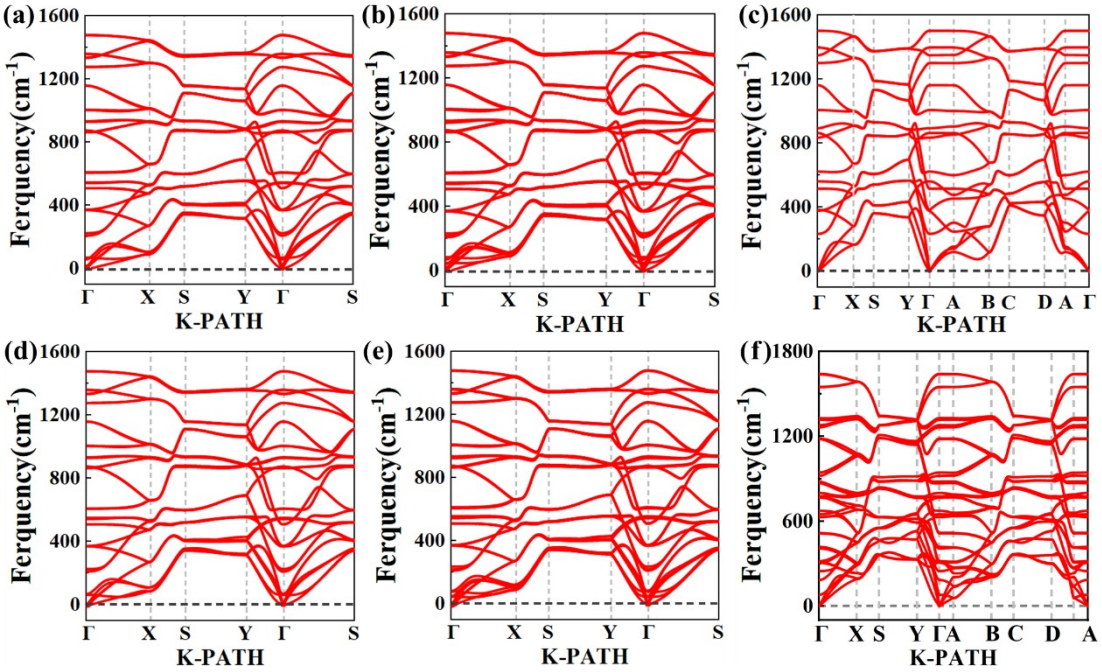

Fig. S4 Calculated phonon spectrum for (a) α-BL, (b) α-TL, (c) α-BK, (d) β-BL, (e) β-TL and (f) β-BK-C_2O, where imaginary part in z direction could be neglected.

Section IV: the basic properties of proposed C_2O-based materials

Table. S1 The calculated lattice parameters (*a* and *b*), the distance between layers (*d*) and the bandgap (E_{PBE} and E_{HSE}) of the layer C_2O-based materials.

	a(Å)	*b*(Å)	*d* (Å)	E_{PBE}(eV)	E_{HSE}(eV)
SL	2.58	4.43	-	3.14	5.01
α-BL	2.58	4.44	1.56	2.97	4.86
α-TL	2.58	4.44	1.55	2.90	4.77
α-BK	2.56	4.44	1.00	2.78	4.49
β-BL	2.58	4.44	1.65	2.98	4.86
β-TL	2.58	4.44	1.64	2.92	4.80
β-BK	2.58	4.45	1.01	1.67	2.83

Table. S2 Predicted Elastic Constants C_{ij} (GPa), Bulk Moduli *B* (GPa), Shear Moduli *G* (GPa), Young's Moduli *E* (GPa) and Poisson's Ratio υ of mentioned 2D materials.

	C_{11}	C_{12}	C_{22}	C_{66}	*B*	*G*	*E*	*υ*	Ref.
Graphene	367.19	69.623	367.19	148.78	218.41	148.78	353.98	0.19	This work
Graphene	349	72	349	138	-	-	334	0.206	Ref.[1]
SL	291.71	23.10	224.51	98.12	140.61	107.81	289.34	0.079	This work
α-BL	582.52	46.55	455.85	197.56	282.87	216.94	577.77	0.080	This work
α-TL	873.36	71.01	688.75	297.34	426.03	326.18	866.04	0.080	This work
β-BL	581.75	45.73	451.57	195.36	281.19	215.41	577.12	0.079	This work
β-TL	872.75	69.10	679.91	292.79	422.72	323.19	865.72	0.079	This work

Table. S3 Predicted Elastic Constants C_{ij} (GPa) of Diamond, α-BK and β-BK.

	C11	C33	C66	C12	C13	Ref.
Graphite	1023	68.46	8.93	263.75	6.26	This work
Graphite	1109	38.7	5	139	0	Ref.[2]
Diamond	1127.69	1127.69	599.56	161.19	161.19	This work
Diamond	1076.00	-	577	125	-	Ref.[3]
α-BK	793.93	358.96	266.04	73.72	-26.09	This work
β-BK	900.80	280.79	150.35	124.57	42.21	This work

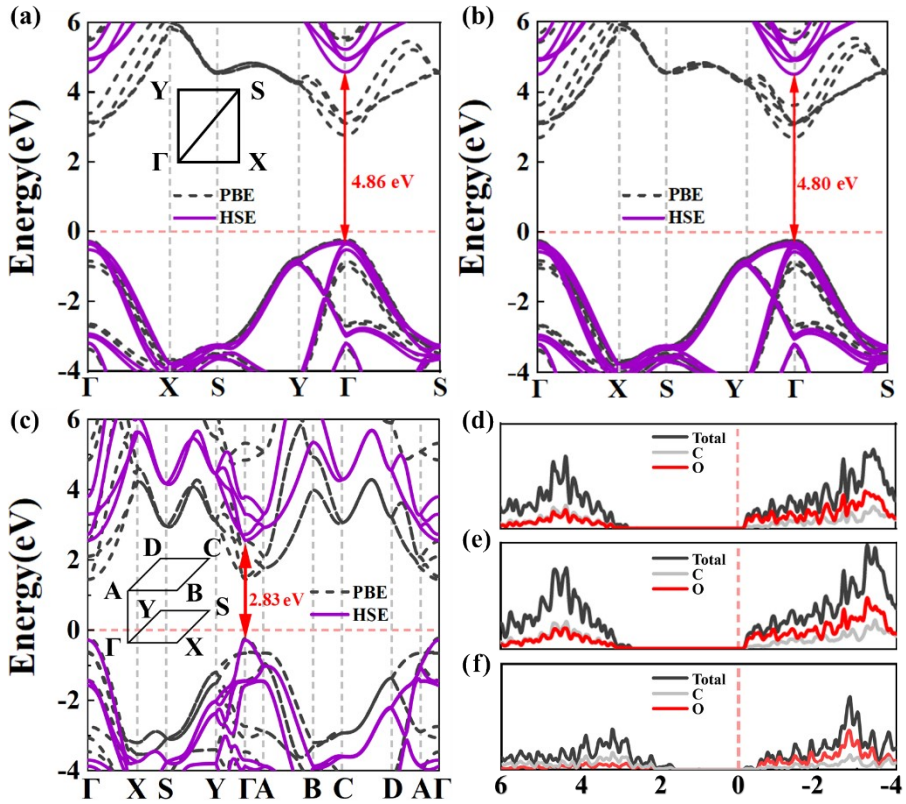

Fig. S5 Band structure of the materials in β-family: (a)BL; (b) TL; (c) BK-C_2O and partial density of states of the materials in β-family: (d)BL; (e) TL; (f) BK-C_2O.

Section V: the mechanical properties of proposed C_2O-based materials

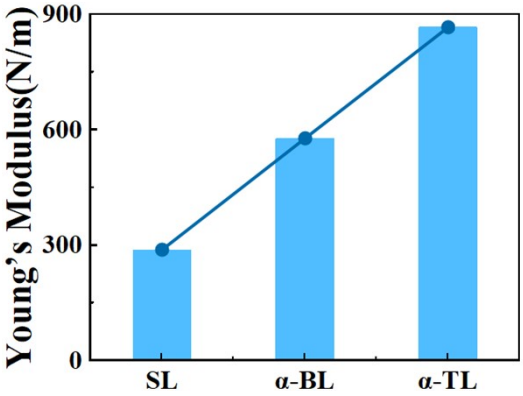

Fig. S6 Young's modulus value along the *x*-direction of SL-C2O, α-BL-C_2O and α-TL-C_2O which is highly linearly correlated.

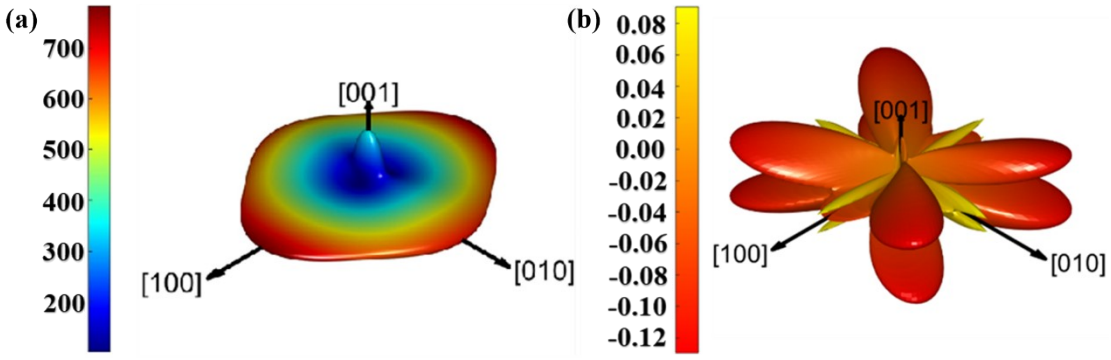

Fig. S7 The overview orientation dependent (a) Young's modulus and (b) the minimum Poisson's ratio of α-BK-C_2O.

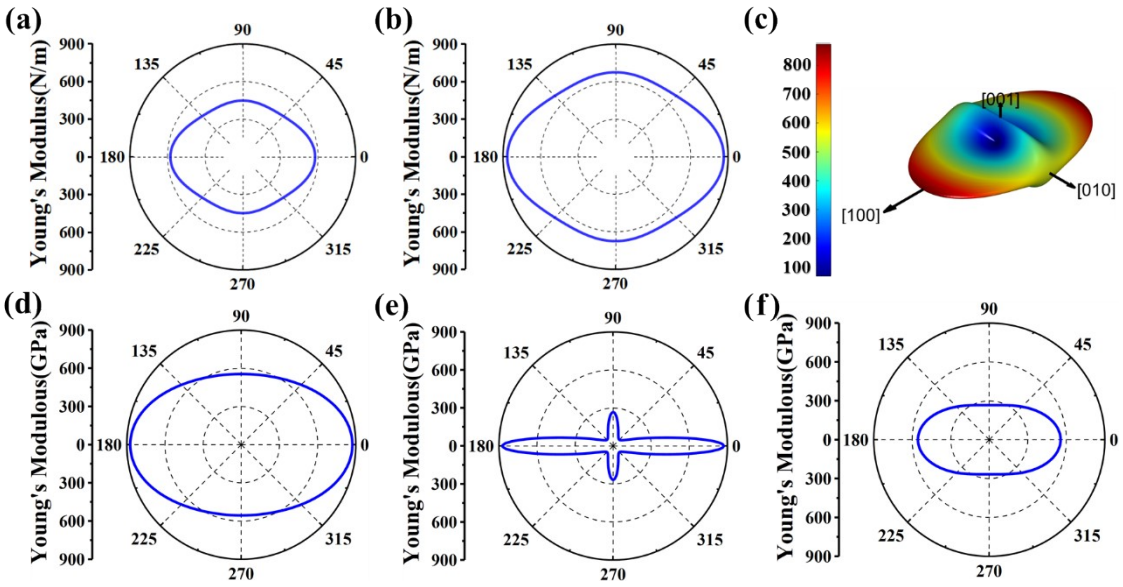

Fig. S8 Orientation dependent Young's modulus of 2D materials and β-BK-C_2O in β-family: (a) β-BL-C_2O; (b) β-TL-C_2O; (c)-(f) the overview of the Young's modulus of β-BK-C_2O and the corresponding axial direction plane (d) *xy*-, (e) *xz*- and (f) *yz*-plane.

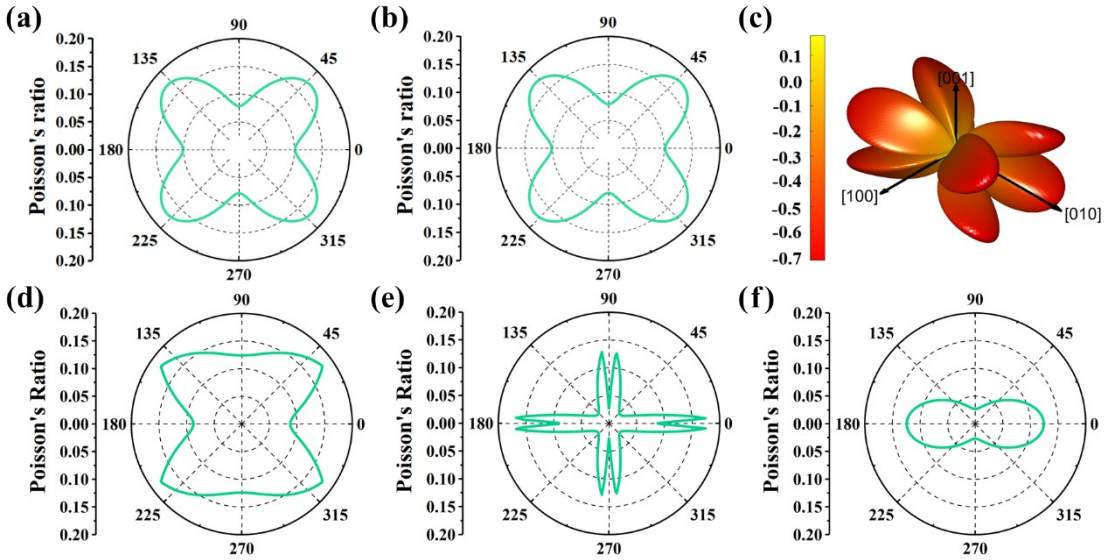

Fig. S9 Orientation dependent Poisson's ratio modulus of 2D materials and β-BK-C_2O: (a) β-BL-C_2O, (b) β-TL-C_2O; and (c)-(f) the overview of the lowest Poisson's ratio of β-BK-C_2O and the corresponding axial directional plane (d) *xy*-, (e) *xz*- and (f) *yz*-plane.

Reference

[1] B. Wang, Q. Wu, Y. Zhang, L. Ma, J. Wang, Auxetic B4N Monolayer: A Promising 2D Material with in-Plane Negative Poisson's Ratio and Large Anisotropic Mechanics, ACS Appl. Mater. Interfaces. 11 (2019) 33231–33237. https://doi.org/10.1021/acsami.9b10472.

[2] K.H. Michel, B. Verberck, Theory of the elastic constants of graphite and graphene, Phys. Status Solidi Basic Res. 245 (2008) 2177–2180. https://doi.org/10.1002/pssb.200879604.

[3] M. H. Grimsditch and A. K. Ramdas, Brillouin scattering in diamond, Physical Review B. (1975) 3139–3148. https://doi.org/10.1103/PhysRevB.11.3139.